Available online at www.sciencedirect.com

ScienceDirect

Procedia Engineering 120 (2015) 245 – 248

Procedia Engineering

www.elsevier.com/locate/procedia

EUROSENSORS 2015

Low temperature gas sensing with novel top-bottom electrode configuration

Azhar Ali Haidry*, Engin Çiftyürek, Bilge Saruhan

Institute of Materials Research, German Aerospace Center (DLR) Linder Hoehe, 51147 Cologne - Germany

Abstract

Gas sensors based on undoped and Cr doped TiO_2 layers with novel top and bottom electrode (TBE) configuration have been employed for NO_2 and H_2 gas sensing. The sensing layers of about 2 micro-meter thickness were sandwiched between 200 nm thick Pt top and bottom electrodes. These sensors with TBE configuration show promising gas sensing behaviour towards both oxidizing and reducing gases. The crystal structure, microstructure and chemical composition studies of the sensors were performed by X-ray diffraction technique (XRD), scanning electron microscopy (SEM) and energy dispersive X-ray spectroscopy (EDX), respectively. The comparative structural, morphological and compositional studies enable us to understand the effect of Cr^{3+} (0.755 Å) substitution within Ti^{4+} (0.745 Å) lattice on gas sensing properties (24°-200°C). The Cr doped TiO_2 sensors were able to detect various concentrations of NO_2 at 200 °C and H_2 at room temperature. Response/recovery times are in the order of tens of seconds for NO_2 at 200 °C and a few minutes for H_2 at room temperature.

Peer-review under responsibility of the organizing committee of EUROSENSORS 2015

Keywords: Titanium dioxide, Cr-doping, NO_2 sensors; TBE electrode configuration; operating temperature

1. Introduction

In recent years gas sensors based on metal oxide semiconductors (MOX) have been aided from the advances in fabrication methods. Generally, MOX (i.e. SnO_2, TiO_2, ZnO, In_2O_3 and NiO) based sensors are fabricated by utilizing the comb-like inter-digital metal electrodes, so-called IDEs, manufactured by screen printing or sputtering

* Corresponding author. Tel.: +492203601-2631, -3228; fax: +492203696480.
E-mail address: Azhar.Haidry@dlr.de; Bilge.Saruhan@dlr.de

Peer-review under responsibility of the organizing committee of EUROSENSORS 2015
doi:10.1016/j.proeng.2015.08.594

techniques to measure electrical conductivity or resistivity. However, selectivity and limited operating temperature range (150°-450° C), depending of sensing material and electrode geometry, are the major issues [1]. In order to provide heating for such sensors a heater, which consume power, must be coupled that thus increases the cost as well as complexity of the sensor device. One way to reduce operating temperature is to prepare nanostructured materials (such as nanotubes, nanowires) for sensing device [2]. Again the complexity of device fabrication increases with incompatibility of such nanostructures with semiconductor industry and their electrode fabrication process that requires sophisticated and expansive techniques (e.g. focused ion beam and e-beam lithography). Another problem with such nanostructured materials based sensors is their long-term stability that fades rapidly with time.

Recently top-bottom electrode (TBE) configuration for TiO_2 thin layer has been reported for room temperature hydrogen sensing with fast response and recovery time [3]. The present work concentrates on both oxidizing (e.g. NO_2) and reducing (H_2) gas sensing behavior of such TBE electrode configuration with Cr-doped TiO_2. The value of potential barrier between grains, regarded as activation energy also ($E_A = eV_s$), is estimated from Arrhenius plots obtained from temperature dependent resistance measurements.

2. Experimental

The sensors with TBE configuration (Fig. 1(a)) were fabricated in three steps: first, 200 nm thick and 300 μm wide bottom Pt electrodes *BE* were patterned (via sputtering) on alumina substrates followed by deposition of 2 μm thick TiO_2 or TiO_2:Cr layers having columnar structures via reactive magnetron sputtering and subsequently perpendicular Pt top electrodes of same dimension as *BE* were patterned. During reactive sputtering of sensing layers, sapphire circular disks (∅ = 13 mm) and silicon (Si) substrates (20×20mm) were also placed side by side for XRD measurements and EDX analysis, respectively, in order to avoid Pt-interference from the inter-digital circuitry and Al from Al_2O_3-substrates. After deposition, the layers were annealed in static air at 800 °C for 3 hour with a heating rate of 6.6 °C / min in a furnace. The width of both top and bottom electrodes were kept fixed in order to fully understand the effect of Cr doping on the sensing mechanism. The crystal structure, surface morphology and chemical composition of the sensing layers were analyzed by X-Ray Diffraction method (XRD), and field emission scanning electron microscope (FE-SEM–Carl Zeiss NTS Ultra 55) equipped with an energy dispersive X-ray (EDX) spectrometer. The structural investigation of the sensors was performed in Bragg-Brantano geometry by using SIEMENS D5000 X-ray Diffractometer with a CuKα radiation (λCuKα = 0.15418 nm) and the graphite curved monochromator. The obtained data was compared with ICSD database via EVA software from BRUKER AXS.

3. Results and Discussion

The thickness and columnar microstructure of the layers were checked by SEM cross-sectional analysis, Fig. 1(b). The thickness of both layers is found to be around 2 μm. Microstructural examination of both coatings exhibits that Cr doped sensing layers are denser with finer columns in comparison to that of undoped TiO_2 layers. The average bottom diameter of undoped TiO_2 (~65 nm) is somewhat smaller than that of Cr-doped TiO_2 (~83 nm). These values are estimated by averaging the diameters of 10 consecutive columns at near bottom as the columns are not uniform in both cases when they reach the surface. In case of undoped TiO_2 the columns non-uniformity is high and tend to combine together at the near surface with voids. The XRD patterns of the undoped TiO_2 and TiO_2:Cr thin layers after annealing at 800°C for 3h are given in Fig 1(c). The XRD spectra of as-deposited coatings, which are not shown here for simplicity purposes, indicate amorphous state. The XRD patterns are presented as the square root of intensity versus 2θ, since the high intensity of the (0006) and (0009) orientations of the sapphire greatly surpass any remaining phases such as anatase (ICSD 01-089-4921) and/or rutile (ICSD 01-088-1172) phase. As Fig. 1(c) reveals, after annealing at 800°C, the coatings contain anatase and rutile phases of TiO_2. Using the weight fraction of rutile phase approximate (W_R) according to [4], the existence of ~63% rutile phase was found in the undoped TiO_2 layers. On the other hand, Cr doping of TiO_2 resulted in a complete anatase to rutile phase transformation. This is in good agreement with the previous literature which mention that the lower valance state dopants can increase the rate of phase transition due to formation of the oxygen vacancies. Powder diffraction characterization of TiO_2:Cr layers showed that all diffraction peaks can be indexed on the basis of the rutile TiO_2 phase (sp. gr. P42/mnm with lattice parameters a=b=4.56 Å, c=2.94 Å) with no appreciable variation in the lattice

parameters due to negligible size effects of dopant material relying on the similarities in ionic radius of the dopant and matrix element. The Cr^{3+} (0.755 Å) ions are potentially to be substituted at Ti^{4+} (0.745 Å) sites within TiO_2 structure [5]. A secondary phase such as Cr_2O_3 was not detected. The grain size of rutile phase TiO_2 and TiO_2:Cr estimated from XRD diffractograms (using standard Scherrer formula) is 8 nm and 4 nm, respectively.

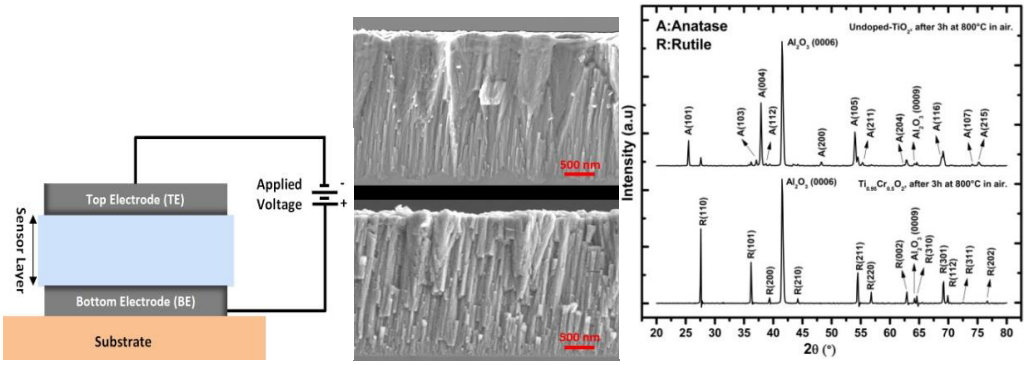

Fig. 1. (a) Schematics of sensors with TBE configuration, (b) SEM cross-section of TiO_2 (top) and TiO_2:Cr (bottom) sensing layers, (c) Comparative XRD diffractograms of both sensors; (b)

An example of the typical dynamic responses of both sensors towards NO_2 (at 200 °C) and H_2 (at room temperature) is shown in Fig. 2. The sensor response for NO_2 (p-type with Cr-doped TiO_2) and H_2 (n-type with Cr-doped TiO_2) gas is defined as $S = R_g/R_b$ and $S = R_b/R_g$, respectively; where R_b is baseline resistance and R_g is saturated resistance in gas. As seen from Fig. 2(a), the Pt/TiO_2/Pt sensors show lower sensor signal towards NO_2 ($S \approx 55$ and 7.5 for C_{NO2} [ppm] = 50 and 100, respectively) with some drift and noise in the signal, while Pt/TiO_2:Cr/Pt sensors show high response ($S \approx 212$ and 545 for C_{NO2} [ppm] = 50 and 100, respectively) with low drift and noise. In case of 1000 ppm hydrogen as given in Fig. 2(b), the response at room temperature is about $S \approx 6.2 \times 10^1$ and 1.03×10^3 for Pt/TiO_2/Pt and Pt/TiO_2:Cr/Pt, respectively. As displayed in Fig. 3(a), response with these sensors is fairly repeatable and reproducible. Meanwhile, the sensors showed decent response τ_{res} and recovery τ_{rec} times for 90% resistance change; for instance τ_{res}&τ_{rec} of TiO_2 and TiO_2:Cr are 10&138 and 37&24 seconds for 100 ppm NO_2 at 200°C and 360&600 and 145&350 seconds under 1000 ppm H_2 at room temperature, respectively. The sensors with IDEs with the same sensing layer showed some response to NO_2 and H_2 above 400 °C.

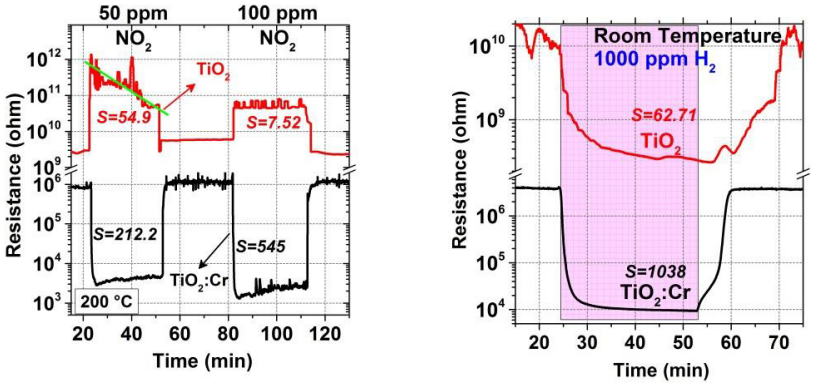

Fig. 2. (a) Comparative dynamic responses of Pt/TiO_2:Cr/Pt and Pt/TiO_2/Pt samples to NO_2 at 200 °C; (b) H_2 at room temperature.

For comparison purposes, the Arrhenius plots of both sensors are plotted using data obtained from resistance versus temperature measurements carried out in synthetic air background, Fig. 3(b). Interestingly nearly similar activation energy E_A value was obtained with both sensors at the temperatures ranging from room temperature to 300 °C. Here the value of E_A represents the height of energy barrier originated between two consecutive grains (R_{air}

= R_0 exp (qV_s/k_bT)), Fig. 3(b). We assume that the grain size 4 nm of the TiO_2:Cr layers is comparable to the Debye Length L_D [6], thus may lead to the complete depletion of the grains in synthetic air background, Fig. 3(b). This agrees with the previous report where authors mentioned that it was anticipated that Cr doping leads to the reduction of Debye length L_D and small grain size which forms localized acceptor levels in forbidden energy gap [7]. Enhanced hydrogen sensing properties has been correlated to complete depletion of the grains [3, 7]. In fact the important issue in *TBE* electrode configuration is the possible interaction of gas with sensing layer through Pt *TE*. Moreover, the overall sensor signal is governed by gas interaction at (i) Pt free sensing surface, (ii) at Pt/MOX interface and (iii) gas diffusion and then reaction with sensing layer below Pt *TE*. Intensive impedance spectroscopy analysis is planned to understand such effects.

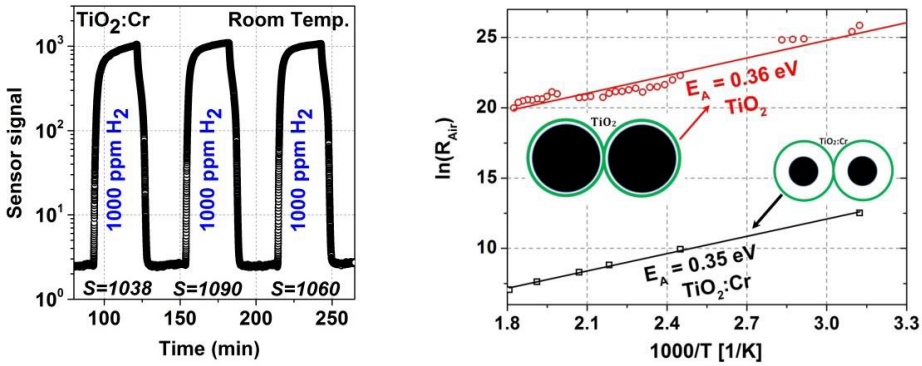

Fig. 3. (a) Consecutive 3 cycle exposure of 1000 ppm H_2 to Cr-doped TiO_2; (b) Comparative Arrhenius plot and depletion at grain size of TiO_2 and TiO_2:Cr sensing layers.

4. Summary and conclusion

In summary, the novel TBE configuration used in this study (Pt/TiO_2 or TiO_2:Cr/Pt) leads to enhancement of NO_2 and H_2 sensitivity. Sensitivity increase is preferentially higher with TiO_2:Cr layers. Moreover, the operating temperature of sensors under exposure to both gases was decreased to as low as 200°C for NO_2 ($S \approx 5.4\times10^2$ to 100 ppm NO_2) and to room temperature for H_2 ($S \approx 1.03\times10^3$ to 1000 ppm H_2). The enhanced sensing properties of Pt/TiO_2:Cr/Pt sensors can be attributed to *TBE* configuration and finer columns with small grain size resulting due to Cr^{3+} integration into TiO_2 lattice. The catalytic role of Pt top electrode causing electron flux through the semiconducting layer needs to be clarified. In order to establish a better understanding of the contribution of various components at the Pt/TiO_2:Cr/Pt sensor configuration and the acceptor type of dopant effect in the electronic structure of the semiconducting oxide layer, intensive impedance spectroscopic investigation is underway.

Acknowledgements

This work has been supported by DAAD-DLR Fellowship Programme under the fellowship number 165 and Helmholtz Postdoc Programme under the contract number of PD-208. The valuable support of Dr. Uwe Schulz, the head of department WF-HFS, is gratefully acknowledged.

References

[1] N. Barsan et al., Metal oxide-based gas sensor research: How to, Sensors and Actuators B 121 (2007), pp. 18 – 35.
[2] G.W. Ho et al., Gas sensor with nanostructured oxide semiconductor materials, Science of Advanced Material 3 (2011), pp. 150 – 168.
[3] T. Plecenik et al. / Sensors and Actuators B 207 (2015) 351–361.
[4] A. A. Gribb and J. F. Banfield, *Am. Mineral,* vol. 82, no. 717, 1997.
[5] J.E. Huheey, Inorganic Chemistry: Principles of structure and reactivity, 3rd edition, Harper Int., New York, 1983, ISBN 0-06-042987-9.
[6] L. G. Teoh et al., Electrochemical and Solid-State Letters, 6 (8) G108-G111 (2003).
[7] B. Lyson-Sypien et al. / Sensors and Actuators B 175 (2012), 163 - 172.